The International Journal of Advanced Manufacturing Technology (2018) 96:1457–1465
https://doi.org/10.1007/s00170-018-1720-8

ORIGINAL ARTICLE

Investigation on the generation of the waviness errors along feed-direction on flycutting surfaces

Chenhui An[1] · Congying Deng[2] · Jianguo Miao[1,3] · Deping Yu[3]

Received: 16 August 2017 / Accepted: 5 February 2018 / Published online: 13 February 2018

Abstract
Ultra-precision single-point diamond flycutting (SPDF) is an irreplaceable technology for cutting KH_2PO_4 (KDP) crystals with large size. However, some undesirable waviness errors along feed-direction exist on the machined surface, which could greatly deteriorate the optical performance of KDP crystals. The spindle dynamic characteristic of SPDF plays an important role in the formation of such waviness errors. This paper presents an on-line measurement method with five-capacitance displacement sensors in nanometer range for monitoring the motion errors of the aerostatic spindle. An error transform theory which is based on kinematic error propagation was introduced to obtain the three-dimensional trajectory of the cutting tool. Then, the spindle motion errors and the cutting tool trajectory were analyzed in frequency domain to investigate the main source of the waviness errors. Simultaneously, the three-dimensional topography of work-piece was simulated by combining the motion trajectory and the geometrical morphology of the cutting tool. The results showed that the waviness errors along feed-direction were caused by the spindle rotation fluctuation with a frequency about 10.8 Hz, and the topography simulations showed good agreement with the machining results. Besides, the experimental results indicated that the error can be diminished by changing the spindle control system to the digital control method. This study established the contact between the measured spindle motion errors and the machined surfaces, which contributes to deeper understanding of the dynamic characteristics of the spindle in SPDF.

Keywords Single-point diamond flycutting · Aerostatic spindle · Topography simulation · Waviness errors

1 Introduction

The potassium dihydrogen phosphate (KDP) crystals are widely used in Inertial Confinement Fusion (ICF) serving as frequency multiplication and pockels cells due to its fine optical properties, such as high leaser-induced damage threshold and fine light transmissivity [1, 2]. However, there are some negative characteristics of the KDP crystals for machining process, such as soft, frangible, anisotropic, and deliquescent. Currently, ultra-precision single-point diamond flycutting (SPDF) is the most useful technology for cutting KDP crystals [3, 4]. The dynamic characteristic of machine tool plays an important role in the machining quality. However, many disturbances, e.g., the environmental disturbance, the structural vibration of the machine tool, the intermittent cutting characteristics, and other undesirable perturbation of the operating parameters, will make the real cutting trajectory of the cutting tool deviate from the ideal cutting trajectory. Thus, machining errors appear on the machined surface, which greatly deteriorates the surface quality and then the optical performance [5].

To achieve better machining quality, lots of efforts have been done to investigate the machining errors in SPDF. Chen et al. [6] quantitatively studied the influence of oil pressure fluctuations on the machined surface in SPDF. They found that the oil pressure is the main source of the waviness errors with a wavelength about 1 mm by surface simulation and experiment validation. Besides, they also investigated the machining errors that are caused by the cutting force fluctuation, the machine tool dynamic characteristics, and the environment vibration in the machining process [7–9]. Li et al. [10] studied the influence of the micro-waviness errors on the damage threshold of the KDP crystals and pointed out that

✉ Congying Deng
dengcy@cqupt.edu.cn

[1] Research Center of Laser Fusion, CAEP, Mianyang 621900, China

[2] School of Adv. Manuf. Eng, Chongqing Univ. of Posts and Telecommunications, Chongqing 400065, China

[3] School of Manufacturing Science and Engineering, Sichuan University, Chengdu 610065, China

the axial vibration of the spindle is the main source to introduce the micro-waviness errors. An et al. [11] analyzed the mid-spatial frequency errors with a wavelength about 100 nm and pointed out that the tilt motion of the spindles is the main cause of the waviness errors by introducing Euler dynamic equations. Yang et al. [12] obtained the cutting tool vibration by combining the dynamic finite element analysis of the aerostatic spindle and the cutting force. They pointed out that the waviness errors along cutting direction are caused by the spindle dynamic characteristics. These researches are beneficial for deeper understanding for the generation of the machining errors in SPDF and indicate that the spindle performance has great influence on the machining errors.

For the spindle, many studies focused on the motion error measurement, the error separation technique, and the simulation [13]. Anandan et al. [14, 15] reported a method to obtain the axial and radial motion errors of an ultra-high-speed miniature spindle by using Laser Doppler Vibrometer. Zhang et al. [16, 17] established a five-degree freedom dynamic model to investigate the translational and tilting motions of an aerostatic spindle and analyzed the natural frequency of the radial, axial, and tilt motions. Chen et al. [18] established a multi-direction error measurement, which uses two master balls to measure the dynamic errors of the spindle. They summarized the frequency characteristics of the main synchronous and asynchronous errors at different rotational speeds. Chen et al. [19, 20] presented a simplified model of the coupled spindle shaft with hydrostatic bearings and identified the main errors of the machine tool based on the wavelet transform.

However, there are few studies investigating the relationship between measured spindle motion errors and machined surface, which would be useful for finding the main sources of the machining errors. In this paper, an on-line five-direction measurement was established to measure the spindle motion errors. And then, an error transform method that suits for SPDF process was introduced to study the cutting tool motion errors which are caused by the aerostatic spindle. Based on that, the main source of a kind of waviness errors along feed-direction was investigated by frequency analysis, and the cutting tool motion errors under different rotation speeds were further studied after optimization.

2 On-line multi-direction measurement setup

The diagram structure of SPDF machine tool is shown in Fig. 1. It can be seen that the SPDF machine tool adopts a gantry structure with a big flycutting head fixed on its spindle bottom. The whole system mainly contains five parts: the aerostatic spindle, the cutting tool, the feeding slide, the work-piece, and the machine tool body. The spindle adopts ultra-precision aerostatic bearing and is driven by a direct current motor with high rotation accuracy. The diamond cutting tool is firmly clamped on the flycutting head edge. The work-piece is fixed on the hydrostatic slide through a vacuum clamp, and the slide is driven by a linear motor with excellent slow feeding performance. All these parts are contacted through the machine tool body.

As shown in Fig. 2, a set of error analyzer produced by Lion Precision Company is adopted to achieve precision measurement. The precision measuring instrument mainly contains five capacitance displacement sensors and a calibrated double master ball (CDMB). And, the whole analyzer system can achieve a minimum resolution about 2 nm. As the spindle system adopts motorized spindle structure, the motor rotor and the spindle are combined through rigid bolts. Meanwhile, the CDMB is firmly connected with the rotor to achieve on-line measurement. Thus, the spindle system and the CDMB can be treated as integration. In flycutting process, the CDMB rotates with the spindle, and the three-dimensional posture of the spindle can be represented by the CDMB. The motion errors of CDMB are measured by the sensors that are fixed in the supporting frame (shown in Fig. 2). One capacity displacement sensor is installed on the supporting frame along the axial direction to measure the axial motion errors. The other four sensors are arranged in two-parallel measuring planes according to CDMB center to measure the radial motion errors and tilting errors.

3 Error transform theory and surface simulation

During SPDF process, the diamond cutting tool rotates with the spindle and directly removes material from the KDP crystals surface. The machined surface is finally determined by the relative motions between the cutting tool and the work-piece surface. According to this cutting mechanism, a kinematic chain of SPDF machine tool is firstly built (shown in Fig. 1). It can be seen that the motion in the cutting tool coordinate system (T) can be transformed to the work-piece coordinate system (W) through the spindle coordinate system (C), the machine tool coordinate system (O), and the feeding slide coordinate system (Y). The relationship between the cutting tool system and the work-piece coordinate system can be described by a transfer matrix ${}^{T}_{W}T$:

$$ {}^{T}_{W}T = {}^{T}_{W}T_{\text{ideal}} \times {}^{T}_{W}E \tag{1} $$

where ${}^{T}_{W}T_{\text{ideal}}$ and ${}^{T}_{W}E$ stand for the ideal transfer matrix and error transfer matrix between the cutting tool coordinate system and the work-piece coordinate system, respectively. And they can be described by the following equations:

$$ {}^{T}_{W}T_{\text{ideal}} = {}^{T}_{C}T_{\text{ideal}} \times {}^{C}_{O}T_{\text{ideal}} \times {}^{O}_{Y}T_{\text{ideal}} \times {}^{Y}_{W}T_{\text{ideal}} \tag{2} $$

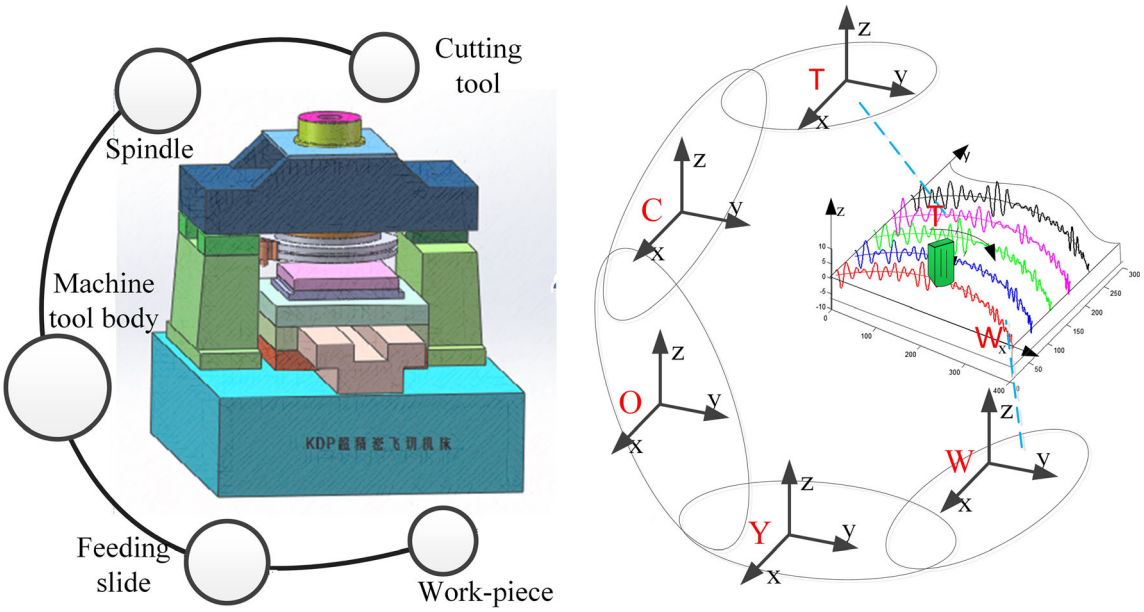

Fig. 1 The diagram structure of SPDF machine tool

$$ {}^{T}_{W}E = {}^{T}_{C}E \times {}^{C}_{O}E \times {}^{O}_{Y}E \times {}^{Y}_{W}E \tag{3} $$

According to that, the actual trajectory of the cutting tool ${}^{T}_{W}S$ in work-piece coordinate system can be obtained by Eq. (4):

$$ {}^{T}_{W}S = {}^{T}_{W}E \times {}^{T}_{W}S_{\text{ideal}} \tag{4} $$

where ${}^{T}_{W}S_{\text{ideal}}$ is the ideal motion of the cutting tool in the work-piece coordinate system. In SPDF, the cutting tool rotates with the spindle and the work-piece achieves feeding motion by the slide. The ideal cutting trajectory of the tool-tip in work-piece coordinate system (W) can be expressed by Eq. (5):

$$ {}^{T}_{W}S_{\text{ideal}} = \begin{bmatrix} R\cos\omega t \\ R\sin\omega t + V_{\text{f}}t \\ z \\ 1 \end{bmatrix} \tag{5} $$

where R is the radius of the flycutting head, ω is the rotation speed of the spindle, V_{f} is the feed speed, and z is the axial location of the cutting tool in work-piece coordinate system.

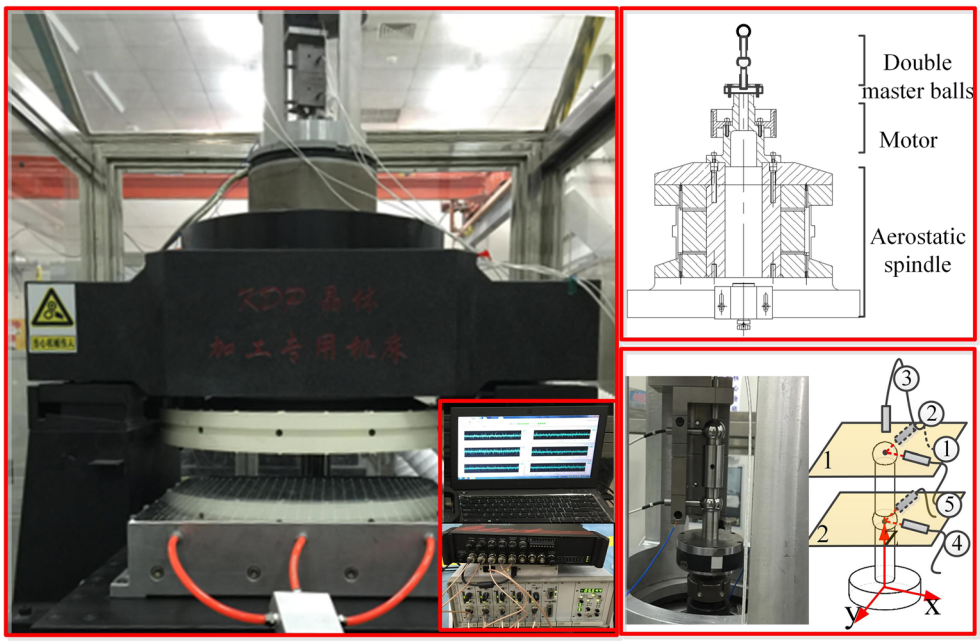

Fig. 2 The on-line multi-direction measurement

The diamond cutting tool is firmly clamped on the flycutting head. Besides, the machine tool body is made of marble, and the vacuum is supported by hydrostatic slide, which both have high stiffness. Thus, ${}^{T}_{C}E$, ${}^{O}_{Y}E$, and ${}^{Y}_{W}E$ can be simply regarded as identity matrix. The real cutting trajectory of the tool-tip in work-piece coordinate system can be expressed by Eq. (6):

$$ {}^{T}_{W}S = {}^{C}_{O}E \times {}^{T}_{W}S_{\text{ideal}} \tag{6} $$

Here, the spindle error motion in W coordinate ${}^{C}_{O}E$ can be expressed by a 4 × 4 matrix:

$$ {}^{C}_{O}E = \begin{bmatrix} {}^{C}_{O}R_{3\times3} & {}^{C}_{O}P_{3\times1} \\ 0_{3\times3} & 1 \end{bmatrix} \tag{7} $$

where ${}^{C}_{O}R_{3\times3}$ and ${}^{C}_{O}P_{3\times1}$ are the rotational transfer matrix and the translational transfer matrix, respectively. And they can be expressed as follows:

$$ {}^{C}_{O}R_{3\times3} = rot(x,\alpha_C) \times rot(y,\beta_C) \times rot(z,\gamma_C) \tag{8} $$

$$ rot(x,\alpha_C) = \begin{bmatrix} 1 & 0 & 0 \\ 0 & \cos\alpha_C & -\sin\alpha_C \\ 0 & \sin\alpha_C & \cos\alpha_C \end{bmatrix} \tag{9} $$

$$ rot(y,\beta_C) = \begin{bmatrix} \cos\beta_C & 0 & \sin\beta_C \\ 0 & 1 & 0 \\ -\sin\beta_C & 0 & \cos\beta_C \end{bmatrix} \tag{10} $$

$$ rot(z,\gamma_C) = \begin{bmatrix} \cos\gamma_C & -\sin\gamma_C & 0 \\ \sin\gamma_C & \cos\gamma_C & 0 \\ 0 & 0 & 1 \end{bmatrix} \tag{11} $$

$$ {}^{C}_{O}P_{3\times1} = \begin{bmatrix} P_{xC} & P_{yC} & P_{zC} \end{bmatrix}^{T} \tag{12} $$

$$ \alpha_C = \arctan\frac{\Delta x_1 - \Delta x_2}{L}, \quad \beta_C = \arctan\frac{\Delta y_1 - \Delta y_2}{L} \tag{13} $$

where α_C, β_C, and γ_C stand for the rotation errors around x-, y-, and z-axes, respectively. $P_{xC} = \Delta x_2$ stands for the translational errors along x-axis, $P_{yC} = \Delta y_2$ stands for the translational errors along y-axis, and $P_{zC} = \Delta z$ stands for the translational errors along the z-axis. Δx_1, Δy_1, Δz, Δx_2, and Δy_2 can be acquired by the five displacement sensors. L is a constant and notes the distance of the two precision balls.

SPDF is an intermittent cutting process. And a circular edge cutting tool with a radius of 5 mm is employed in SPDF. Therefore, the work-piece surface generation along feed-direction is determined by cutting interference phenomenon. The height z of a certain position $P(x, y)$ is influenced by several close intermittent cuttings which can be expressed by the following equations:

$$ y_n = R - \sqrt{R^2 - x^2} + f \cdot \frac{\arcsin(x/R)}{\omega} + Y_n \tag{14} $$

$$ z_n = R_T - \sqrt{{R_T}^2 - (y - y_n)^2} \tag{15} $$

$$ z = \min(z_n) \tag{16} $$

where Y_n is the initial y location of several close intermittent cutting trajectories, z_n is the height under the influence of several close intermittent cutting trajectories, and R_T is the radius of the cutting tool. The surface simulation can be carried out by combining the tool-tip cutting trajectory, the cutting interference phenomenon and the displacement of the cutting tool influenced by the spindle motion errors.

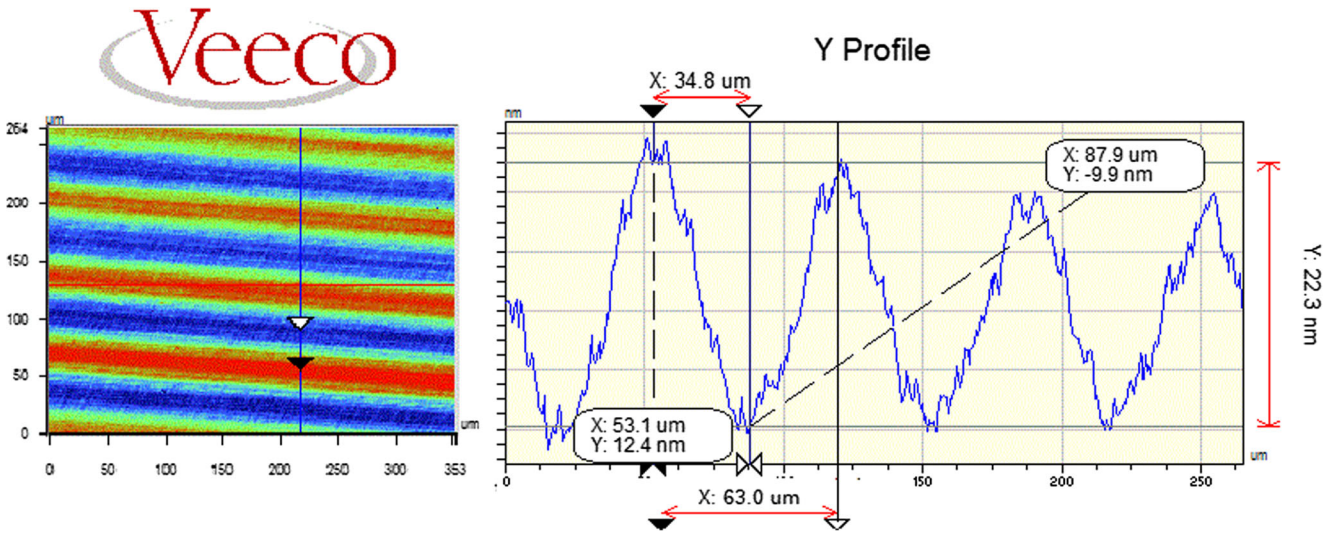

Fig. 3 The measured three-dimensional topography and two-dimensional profile of the waviness errors along feed-direction

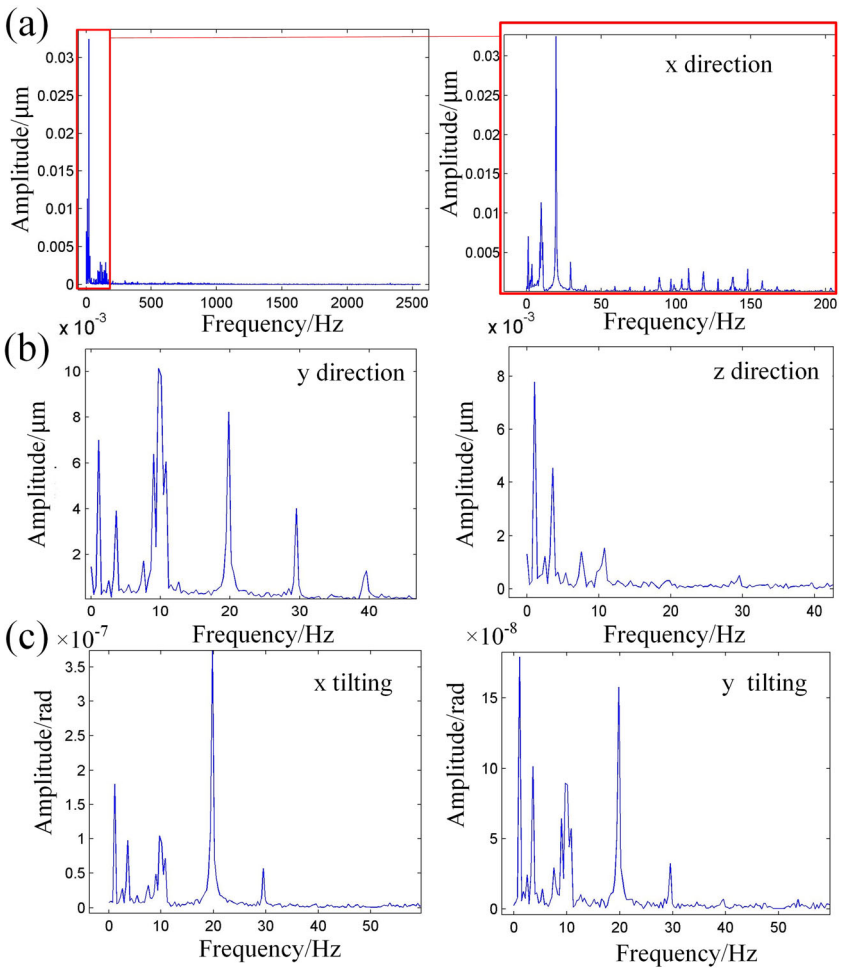

Fig. 4 The frequency characteristics of the spindle motion errors. (**a**) spindle motion errors along *x* direction, (**b**) spindle motion errors along *y* and *z* directions, and (**c**) spindle tilting errors

4 Experimental results and discussions

The working condition plays an important role in SPDF process. In this paper, all of the experiments with the special SPDF are carried out in clean room, in which the temperature is precisely controlled at about 21 °C and the humidity is maintained at a stable level about 20%. Simultaneously, the SPDF machine tools are specially placed on the vibration isolation ground to minimize the environmental disturbance. However, some waviness errors along feed-direction were found on the machined KDP crystal surface recently while a profiler ZYGO NEWVIEW 7200 (minimum measurement better than 1 nm) was used to measure the surface topographies. It should be noted that the crystals are machined under the following cutting parameters: cutting depth of 2 μm, feed rate of 60 μm/s, and rotation speed of 590 rpm. Here, the waviness errors appear despite of the rotation speed, and 590 rpm is just selected as an example. The measured three-dimensional topography and 2D profile of the machined surface are shown in Fig. 3. It can be seen that amplitude of the

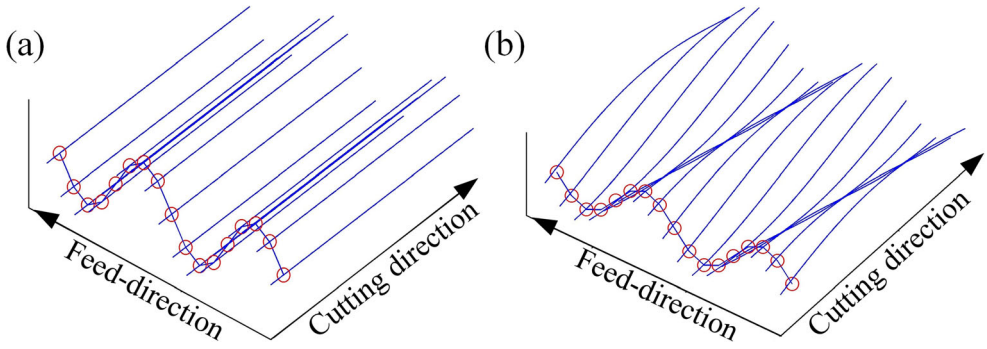

Fig. 5 The influence mechanism of two different frequencies (**a**) influence mechanism of 1.1 Hz motion errors and (**b**) influence mechanism of 10.8 Hz motion errors

micro-waviness errors is about 22 nm, and the wavelength is about 63 μm (time period about 1 s). These waviness errors will deteriorate the optical performance of the KDP crystals, and the main source should be identified.

In SPDF, the spindle directly influences the real cutting trajectory of the cutting tool. Therefore, the motion errors of the spindle are measured using the mentioned on-line measurement to study the main source of the waviness errors. The waviness errors possess strict periodicity. Thus, the key attention is paid to the frequency characteristics which are analyzed by FFT method. The frequency components of the radial errors in two measure planes are similar. Hence, the measured results in the upper plane are selected to represent the radial motion errors.

The frequency characteristics of radial errors along x direction, y direction, and the axial errors along z direction are presented in Fig. 4a, b; it can be seen that the main frequency components are below 50 Hz, which indicates that the low frequency plays dominating roles in the spindle motion errors and should be paid more attention to. Besides, it can be found that the main components of the low frequency along x, y, and z direction are similar. And they all possess dominating frequencies of 19.8, 1.1, 9.7, and 10.8 Hz, which greatly influence the spindle motion and the machined surface. The frequency characteristic of the spindle tilting errors is shown in Fig. 4c; it can be found that the main components of the titling motion are also accordant with the radial results, and the dominating frequencies are 19.8, 1.1, 9.7, and 10.8 Hz. Among these four main frequencies, 9.7 and 19.8 Hz are the onefold and twofold frequencies of the rotation frequency, respectively. They both belong to synchronous errors and can make the real cutting location deviate from the ideal cutting location. However, the deviation of the cutting location can be neglected because of the same vibration phase along feed-direction, which cannot generate the mentioned waviness errors.

Table 1 The main frequencies of the cutting tool motion errors

Errors	1st	2nd	3rd	4th	5th	6th
Radial x	19.8	1.1	9.7	9	10.8	3.6
Radial y	9.7	19.8	1.1	9	10.8	29.5
Axial z	1.1	3.6	96	104	10.8	7.6
Tilting x	19.8	1.1	9.7	3.6	10.8	9
Tilting y	1.1	19.8	3.6	9.7	9	10.8
Total axial	29.5	9.7	19.8	8.8	10.9	13.3

The main frequency of 1.1 and 10.8 Hz belong to the asynchronous errors, and their influence on the surface generation in SPDF can be calculated by the transform model. Setting the rotation frequency and asynchronous frequency as f_R and f_E, respectively. The asynchronous errors can be expressed by Eq. (17):

$$Z = \Delta z \sin(2\pi f_E t + \varphi) \tag{17}$$

where Δz notes the error amplitude. The phase will increase $\Delta\varphi$ per revolution, and it can be described by Eq. (18). The waviness errors along feed-direction will generate when the phase increase to 2π after several revolutions. Besides, the

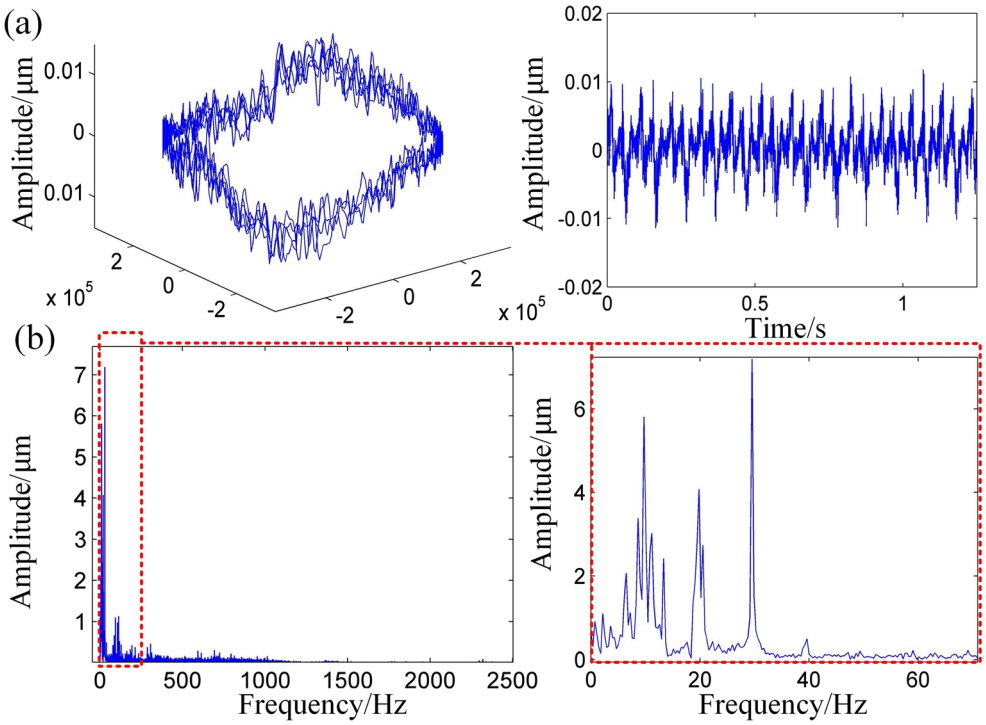

Fig. 6 The dynamic characteristics of the cutting tool, (**a**) cutting trajectory, and motion errors (**b**) frequency characteristics

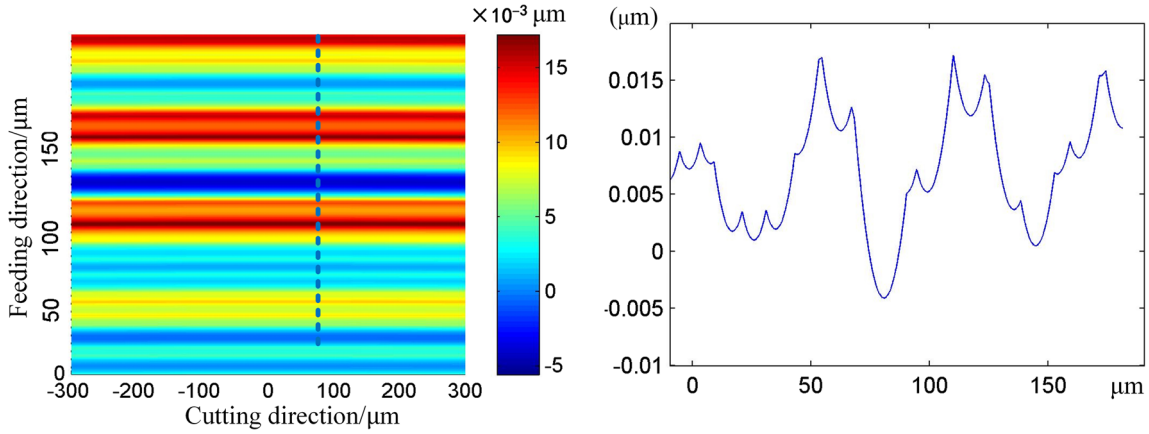

Fig. 7 The three-dimensional topography and two-dimensional profile of the simulated surface

period and wavelength of the waviness errors can be described by Eq. (19):

$$\Delta\varphi = 2\pi\left(\frac{f_E}{f_R} - N\right) \tag{18}$$

$$T = \frac{1}{|Nf_R - f_E|}, \quad L_w = \frac{V_f}{|Nf_R - f_E|} \tag{19}$$

where N notes the closest inter of f_E/f_R, and V_f notes the feeding speed. The frequency 1.1 Hz is specially fit for the situation that $N = 0$, and the influence mechanism can be explained by Fig. 5a. The frequency 10.8 Hz is fit for the situation that $N = 1$ and the influence mechanism can be expressed by Fig. 5b. Therefore, both of the two asynchronous errors are likely to generate the waviness errors along feed-direction, which needs further analyzed.

Then, the measured results of multi-direction errors are substituted into the transform model to obtain the trajectory and the axial motion errors of the cutting tool (shown in Fig. 6a). The frequency characteristics of the cutting tool motion errors are further shown in Fig. 6b, and the top six frequencies of the spindle motion errors that have dominating influence are summarized in Table. 1. It can be found that the main asynchronous errors with frequency of 1.1 Hz disappear while the 10.8 Hz still exist. Above all, the main source of the waviness errors along feed-direction is the asynchronous errors with frequency about 10.8 Hz.

The surface simulation considering the motion errors of the cutting tool is shown in Fig. 7. It is clear that surface simulation obtained the waviness errors along the feed-direction. The wavelength of the simulated waviness errors is about 60 nm, and the peak-to-valley value of the two-dimensional profile is about 20 nm which is well coincident with the experimental waviness errors. Thus, it validates that spindle motion errors are the main source of the waviness errors along feed-direction and the surface simulation based on on-line multi-direction measurement can achieve well prediction of the machined surface in SPDF.

As the spindle system adopts motorized spindle structure, the performance of motor directly influences the spindle motion

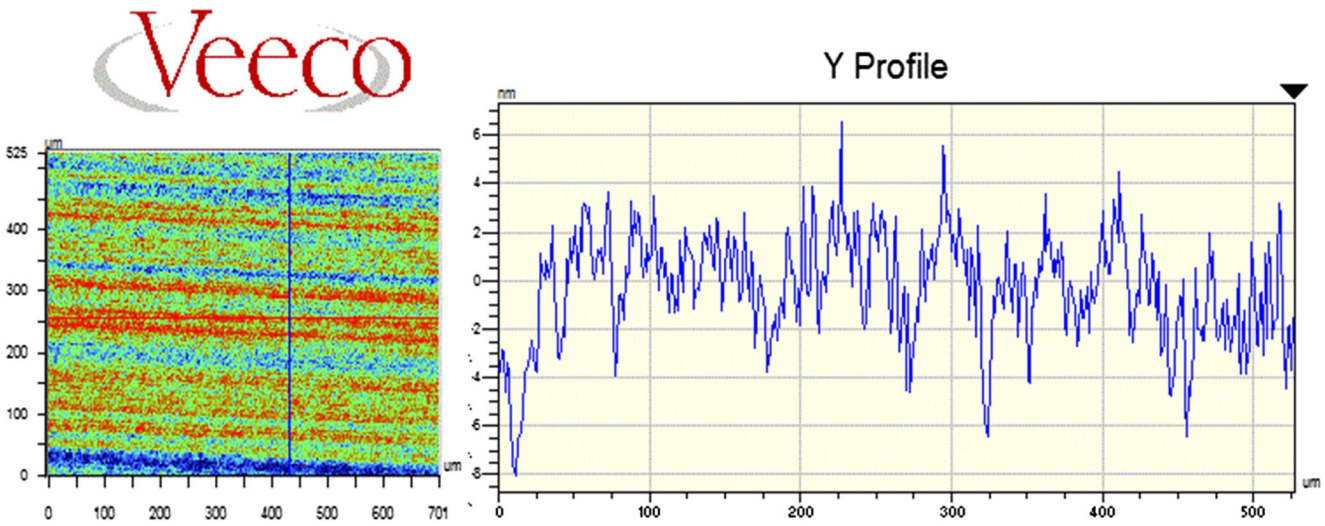

Fig. 8 The measured surface topography after optimization

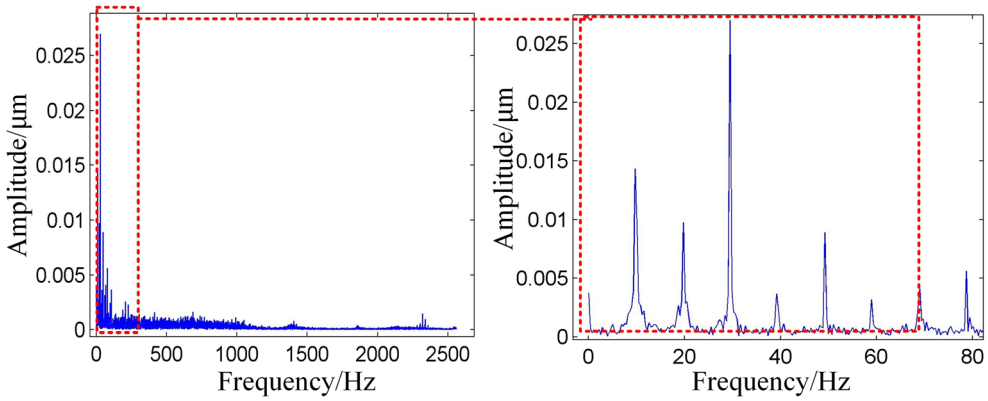

Fig. 9 The frequency characteristics of the cutting tool motion errors after optimization

errors. The motor is controlled by analog control system which is easier to be disturbed and may generate rotation fluctuation when compared to digital control system. Thus, a method is adopted by using the digital control system to restrain the generation of the waviness errors. Experiments are carried out under the aforementioned cutting parameters to demonstrate the effectiveness of the digital control method. The machined result is shown in Fig. 8. It can be found that the waviness has been significantly restrained and the peak-to-valley value of the two-dimensional profile has decreased from 20 to 10 nm. Simultaneously, the frequency of the cutting tool motion errors is analyzed and the result is shown in Fig. 9. It can be seen that the asynchronous errors with frequency about 10.8 Hz disappear. The experimental results clarify that the spindle rotation fluctuation, which is introduced by the analog control system, is the main source of the mentioned waviness errors along feed-direction. And the waviness errors can be evidently restrained by using digital control method.

In order to guide the practical processing and reduce exploration cost, experiments are carried out to study the motion errors of the cutting tool by combining the on-line multi-direction measurement and the error transform model. The RMS of the radial motion errors under different rotation speeds are shown in Fig. 10. It can be found that the total radial motion errors decrease at first and then tend to be stable with the increase of the rotation speed. And the total radial errors tend to increase slightly when the rotation speed exceeds 400 rpm. The radial asynchronous errors decrease with the increase of the rotation speed while the radial synchronous errors increase when the rotation speed exceeds 600 rpm, which means too high rotation speed is not conducive to the machining quality improvement due to the increased vibration.

The RMS of the axial motion errors under different rotation speeds are shown in Fig. 11. It can be found that the total axial motion errors are larger than the radial motion errors, which mean the axial motion errors play dominating role in the surface generation in SPDF. The total axial motion errors decrease at first and then tend to be stable with the increase of the rotation speed. The axial asynchronous error decreases with the increase of the rotation speed while the axial synchronous errors have little increase when the rotation speed exceeds 400 rpm.

Above all, the cutting motion errors are relative small both in radial and axial direction when the rotation speed is set between 430 and 450 rpm, which contributes to improving the surface quality in SPDF.

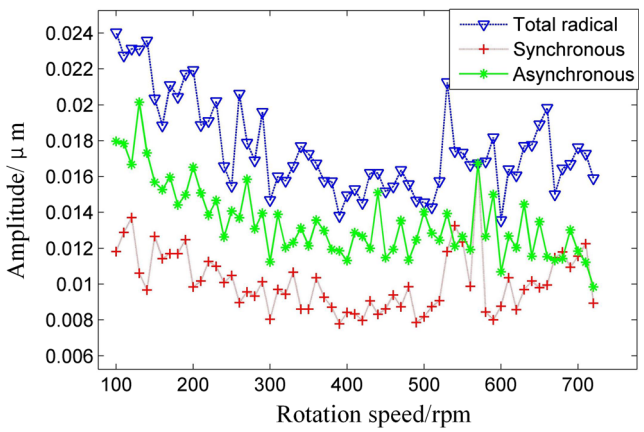

Fig. 10 RMS of the radial motion errors under different rotation speeds

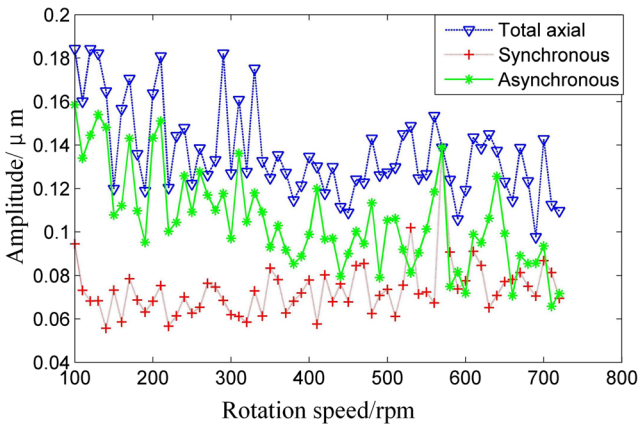

Fig. 11 RMS of the axial motion errors under different rotation speeds

5 Conclusions

In this paper, an on-line multi-direction measurement and an error transform model are combined to investigate the main source of the waviness errors along feed-direction based on frequency analysis. The motion errors of the cutting tool at different rotation speeds are further studied after optimization. The following conclusions can be drawn from the study:

1. The method combining the on-line multi-direction measurement, the error transform model, and frequency analysis is effective in investigating the waviness errors in SPDF. And this method is useful for studying the motion errors in different conditions.
2. The spindle rotation fluctuation, which is caused by the analog control system, is determined to be the main source of the waviness errors along feed-direction. And changing the control system of the spindle from analog to digital control can effectively eliminate the waviness errors.
3. The motion errors both in the radial and axial directions are relatively small when the rotation speed is set between 430 and 450 rpm, which contributes to better surface quality in SPDF.

Funding information This research was supported by the Science Challenge Project (no. JCKY2016212A506-0504) and the Science and Technology Research Program of Chongqing Municipal Education Commission (no. KJ1704087).

References

1. Burkhart SC, Bliss E, Di NP, Kalantar D, Lowe-Webb R, Mccarville T (2011) National ignition facility system alignment. Appl Opt 50(8):1136–1157
2. Moses EI (2008) The national ignition facility and the golden age of high energy density science. Pulsed Power Conference, IEEE Int 36:16–19
3. Chabassier G (1999) Using a design of experiment method to improve KDP crystal machining process 3492:814–820
4. Liang YC, Chen WQ, Bai QS, Sun YZ, Chen GD, Zhang Q, Sun Y (2013) Design and dynamic optimization of an ultraprecision diamond flycutting machine tool for large KDP crystal machining. Int J Adv Manuf Technol 69(1):237–244
5. Sun YZ, Chen WQ, Liang YC, An CH, Chen GD, Su H (2015) Dynamic error budget analysis of an ultraprecision flycutting machine tool. Int J Adv Manuf Techol 76(5):1215–1224
6. Chen WQ, Liang YC, Sun YZ, An CH, Chen GD (2014) Investigation of the influence of constant pressure oil source fluctuations on ultra-precision machining. Proc Instit Mech Eng Part B: J Eng Manuf 229(2):372–376
7. Chen WQ, Sun YZ, An CH, Su H, Yang K, Zhang Q (2015) Modeling and simulation of the interaction of manufacturing process and machine tool structure in flycutting machining. Proc Instit Mech Eng Part C: J Eng Sci 229(15):2730–2736
8. Liang YC, Chen WQ, An CH, Luo XC, Chen GD, Zhang Q (2013) Investigation of the tool-tip vibration and its influence upon surface generation in flycutting. Proc Instit Mech Eng Part C: J Eng Sci 228(12):2162–2167
9. Sun YZ, Chen WQ, Liang YC, An CH, Chen GD, Su H (2014) An integrated method for waviness simulation on large-size surface. Proc Instit Mech Eng Part B: J Eng Manuf 229(1):178–182
10. Li MQ, Chen MJ, An CH, Zhou L, Cheng J, Xiao Y, Jiang W (2012) Mechanism of micro-waviness induced KH2PO4 crystal laser damage and the corresponding vibration source. Chinese Phys B 21(5):34–42
11. An CH, Zhang Y, Xu Q, Zhang FH, Zhang JF, Zhang LJ, Huang JH (2010) Modeling of dynamic characteristic of the aerostatic bearing spindle in an ultra-precision fly cutting machine. Int J Mach Tools Manuf 50(4):374–385
12. Yang X, An CH, Wang ZZ, Wang QJ, Peng YF, Wang J (2016) Research on surface topography in ultra-precision flycutting based on the dynamic performance of machine tool spindle. Int J Adv Manuf Technol 2016:1–9
13. Lee JC, Gao W, Shimizu Y, Hwang J, Oh JS, Park CH (2012) Spindle error motion measurement of a large precision roll lathe. Int J Precis Eng Manuf 13(6):861–867
14. Anandan KP, Ozdoganlar OB (2013) Analysis of error motions of ultra-high-speed (uhs) micromachining spindles. Int J Mach Tools Manuf 70(7):1–14
15. Anandan KP, Tulsian AS, Donmez A, Ozdoganlar OB (2011) A technique for measuring radial error motions of ultra-high-speed miniature spindles used for micromachining. Precis Eng 36(1): 104–120
16. Zhang SJ, To S, Cheung CF, Wang HT (2012) Dynamic characteristics of an aerostatic bearing spindle and its influence on surface topography in ultra-precision diamond turning. Int J Mach Tools Manuf 62(1):1–12
17. Zhang SJ, To S, Zhang GQ, Zhu ZW (2015) A review of machine-tool vibration and its influence upon surface generation in ultra-precision machining. Int J Mach Tools Manuf 91:34–42
18. Chen GD, Sun YZ, An CH, Zhang FH, Sun ZJ, Chen WQ (2016) Measurement and analysis for frequency domain error of ultra-precision spindle in a flycutting machine tool. Proceedings of the Institution of Mechanical Engineers. Part B: J Eng Manuf
19. Chen DJ, Gao X, Dong LH, Fan JW (2016) An evaluation system for surface waviness generated by the dynamic behavior of a hydrostatic spindle in ultra-precision machining. Int J Adv Manuf Technol 91(5–8):2185–2192
20. Chen DJ, Zhou S, Dong LH, Fan JW (2016) An investigation into error source identification of machine tools based on time-frequency feature extraction. Shock Vib 2016:1–10